

# Alternative Load Path Analysis of a Prototype Reinforced Concrete Frame Building

Yihai Bao<sup>1</sup>, Joseph A. Main<sup>2</sup>, and H.S. Lew<sup>3</sup>

Engineering Laboratory, National Institute of Standards and Technology  
100 Bureau Drive, Mail Stop 8611, Gaithersburg, MD 20899-8611

<sup>1</sup>Tel: (301) 975-2061; E-mail: yihai.bao@nist.gov

<sup>2</sup>Tel: (301) 975-5286; E-mail: joseph.main@nist.gov

<sup>3</sup>Tel: (301) 975-6060; E-mail: hai.lew@nist.gov

## ABSTRACT

This paper presents alternative load path analysis of a 5-bay by 5-bay, 10-story prototype reinforced concrete moment frame building under column loss scenarios. This prototype building is used for example analysis problems in the *Alternative Load Path Analysis Guidelines*, which are being developed by the Disproportionate Collapse Technical Committee of the Structural Engineering Institute, and the analyses presented in this paper have been submitted for inclusion in these guidelines as part of the chapter on advanced numerical modeling. The prototype building was designed for seismic design category C, for a location in Atlanta, GA. Intermediate moment frames were selected as the lateral force-resisting system and were designed in accordance with the requirements of the American Concrete Institute 318 Building Code. A two-way concrete slab was used at each floor level, including the roof. Using a reduced-order finite-element modeling approach, full-building analyses are presented under three different first-story column loss scenarios, including a corner column, an edge column, and an interior column. Results from nonlinear dynamic analysis (i.e., sudden column removal) are compared with results from nonlinear static analysis (i.e., push-down analysis) using an energy-based procedure to account for the dynamic effects of sudden column loss. The robustness index for the building is also evaluated based on its ultimate capacity under the same set of sudden column loss scenarios.

## INTRODUCTION

Alternative load paths in a structural system enable redistribution of loads after failure of a load-bearing member, thus preventing a progression of failures that could result in disproportionate collapse. Alternative load path analysis (ALPA) is a commonly accepted approach for evaluating the susceptibility of a structure to disproportionate collapse. A key first step in ALPA is the selection of appropriate initial damage scenarios. Multiple scenarios involving removal of load-bearing members must generally be considered to determine the most critical scenarios for design. Structural analysis is then performed to evaluate the adequacy of the structural members and connections to develop alternative load paths within specified strength and deformation limits. The Disproportionate Collapse Technical Committee of the Structural Engineering Institute is currently developing guidelines for performing ALPA. These

guidelines present alternative modeling and analysis approaches that are categorized within three different levels of complexity: 1) simple mechanics-based hand- and spreadsheet- calculable methods, 2) analysis methods using structural analysis and design software, and 3) advanced numerical modeling and analysis methods. This paper presents ALPA approaches and examples for a reinforced concrete frame building that fall within the third category of advanced numerical modeling and analysis.

The modeling and analysis approaches presented in this paper are illustrated using example analysis problems from the *ALPA Guidelines* that correspond to a 10-story, 5-bay by 5-bay reinforced concrete moment frame building with a two-way concrete slab at each floor level. Three first-story column removal scenarios are analyzed, including removal of a corner column, an edge column, and an interior column. A reduced-order finite-element modeling approach is used, in which the beams and columns are modeled with beam elements, the slab is modeled using shell elements, and special interface beam elements are used to model bond slip and reinforcing bar fracture at critical beam sections. The reduced-order modeling approach captures important geometrically nonlinear response mechanisms such as arching action, catenary action, and slab membrane action. The material modeling considers nonlinear behavior and accounts for key effects such as concrete confinement, concrete damage and softening, bond slip of reinforcing bars, and reinforcing bar fracture. An approximate energy-based procedure is employed to demonstrate that the dynamic effects associated with sudden column loss can be evaluated from the results of a nonlinear static push-down analysis. Finally, the robustness index of the prototype building is calculated based on the ultimate capacities of the prototype building obtained from nonlinear static analysis under the set of column removal scenarios.

## **PROTOTYPE BUILDING**

Fig. 1 shows elevation and plan views of the prototype reinforced concrete frame building. The building has a rectangular plan with five bays in each direction and a typical bay size of 9.1 m (30 ft) by 6.1 m (20 ft). There are no interior columns along gridlines 2 and 5, resulting in 12.2 m (40 ft) spans for the north-south interior girders that frame into the exterior columns. The first-story height is 4.6 m (15 ft), and the height of each upper story is 3.7 m (12 ft).

The building was designed for the combined effects of gravity and lateral loads as specified by the American Society of Civil Engineers (ASCE) Standard 7-02 (ASCE 2002). The gravity loads included self-weight, superimposed dead load, and live load, with values listed in Table 1 for typical floors and for the roof. For typical floors, live load reduction was considered based on Section 1607.9.1 of the International Building Code (ICC 2003). Wind and seismic loads were considered for a location in Atlanta, GA, for seismic design category C. The lateral loads are resisted by intermediate moment frames designed using the American Concrete Institute (ACI) 318-02 code (ACI 2002). A two-way normal-weight concrete slab with a thickness of 254 mm (10 in) was used for all floor levels, including the roof. Normal-weight concrete with a nominal compressive strength of 27.6 MPa (4000 psi) was used for all structural members. All reinforcing bars had a minimum specified yield strength of 414 MPa (60 ksi). Additional details on the design of the building are provided by Shen and Ghosh (2006).

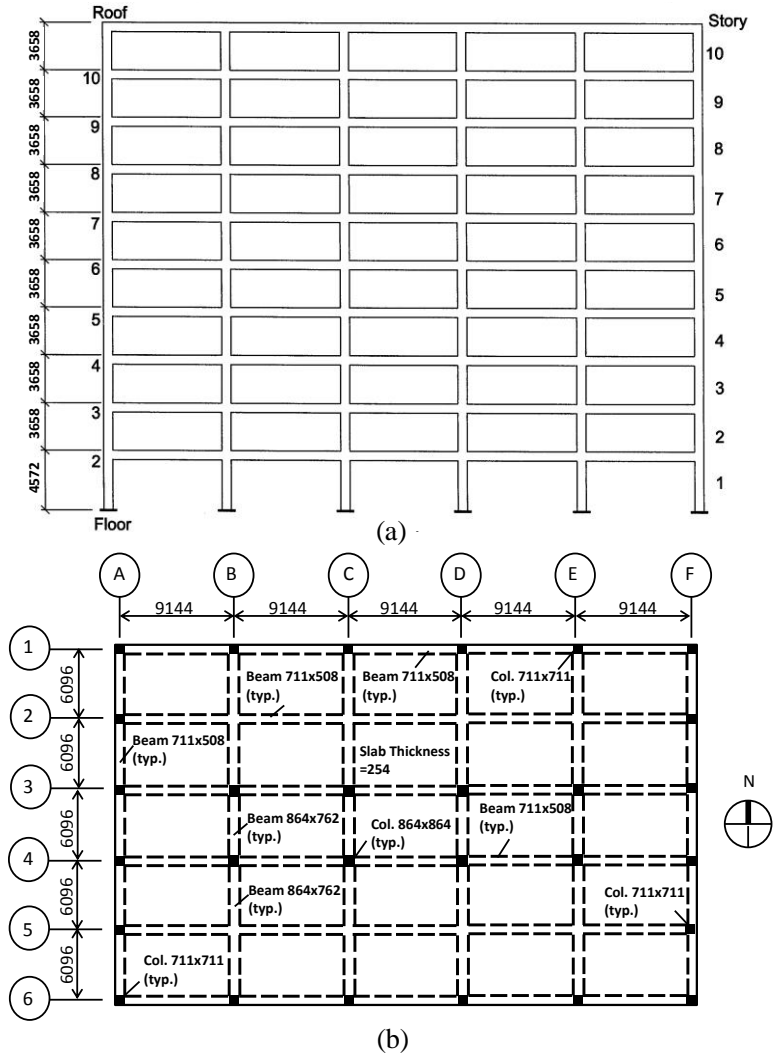


**Fig. 1. Prototype concrete frame building: (a) elevation view and (b) plan view. (dimensions in mm)**

**Table 1. Gravity loads for prototype building.**

Gravity Load Type	Load Intensity, kN/m <sup>2</sup> (lbf/ft <sup>2</sup> )	
	Typical Floors	Roof
Self-weight	7.18 (150)	7.18 (150)
Superimposed dead load	1.44 (30)	0.48 (10)
Total dead load, <i>D</i>	8.62 (180)	7.66 (160)
Live load, <i>L</i>	4.79 (100)	1.20 (25)

## MODELING APPROACH

As described in the following subsections, the prototype building was modeled using a reduced-order finite-element approach in which the beams and columns were modeled using beam elements and the slab was modeled using shell elements. Nonlinear material behavior was considered for the concrete and the steel reinforcement, and special interface beam elements were used to model bond slip and reinforcing bar fracture at critical beam sections. The LS-DYNA finite element software<sup>1</sup> (LSTC 2014) was used for the modeling and analysis in this study.

**Reduced-order modeling of framing members and slabs.** The reduced-order modeling approach used in this study, illustrated in Fig. 2, is a modified version of the approach presented previously by Bao et al. (2014b), with two notable simplifications:

- (1) Joint shear deformations, which were considered by Bao et al. (2014b), were neglected in this study, since they were found to have an insignificant influence on the nonlinear response of the structure under column loss scenarios. The joints were modeled using rigid links with lengths corresponding to the dimensions of the joint region, as illustrated in Fig. 2.
- (2) Nodes of the beam and shell elements, which were defined in different planes by Bao et al. (2014b), were defined in a common plane at the top surface of the slab in this study, thus simplifying the model development. Offsets were used to define the reference axes of the elements at their proper elevations, and nodal constraints were used to tie the beam elements to the shell elements, ensuring continuity of displacements and rotations at the interface between the beams and the floor slab (see Fig. 2).

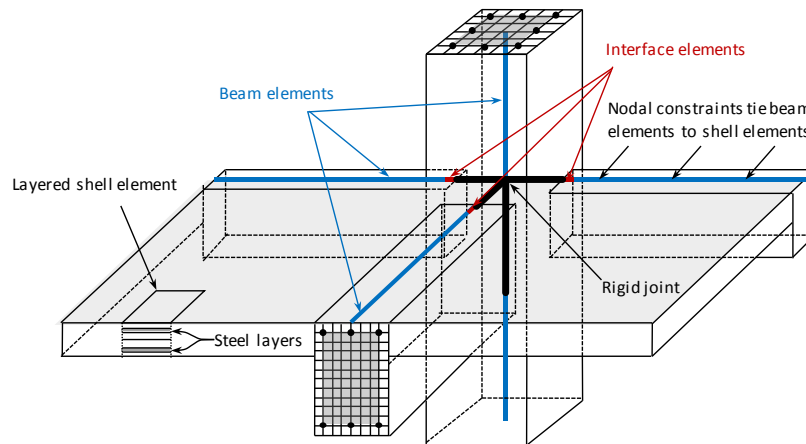


**Fig. 2. Reduced-order model for RC frame building including floor slab**

---

<sup>1</sup> Certain commercial entities or products are identified in this document in order to describe a procedure or concept adequately. Such identification is not intended to imply recommendation or endorsement by the National Institute of Standards and Technology, nor is it intended to imply that the entities or products are necessarily the best available for the purpose.

The floor slabs were modeled using layered shell elements with through-thickness integration, with distinct layers representing concrete and reinforcing steel. The beams and columns were modeled using Hughes-Liu beam elements with cross-section integration (Hallquist 2007), with distinct integration points for cover concrete, core concrete (for which confinement effects were considered as discussed in the following subsection), and reinforcing steel. Bond slip at critical cross sections, including the beam-to-column interfaces and the bar cut-off locations, was considered by using special interface elements (beam elements with cross-section integration) with a modified stress-strain relationship for the reinforcing bars that incorporated displacements due to bond slip, as discussed subsequently.

**Material modeling.** The material stress-strain relationships used in the analyses are illustrated in Fig. 3. Expected-strength material properties, rather than lower-bound material properties, were used in the analyses, as listed in Table 2. Expected strength factors from Table 10-1 of ASCE 41-13 (ASCE 2013) were used to translate lower-bound material properties to the expected-strength properties listed in Table 2, with an expected strength factor of 1.50 for the concrete compressive strength  $f'_c$  and a factor of 1.25 for the yield strength  $f_y$  and tensile strength  $f_u$  of reinforcing steel. The concrete tensile strength was calculated from the compressive strength according to the CEB-FIP model code (CEB 1991). The steel reinforcement was assumed to be ASTM A706, Grade 60, which has a minimum specified yield strength of 414 MPa (60 ksi) and a minimum specified tensile strength of 552 MPa (80 ksi).

For the reinforcing steel (Fig. 3(a)), the modulus of elasticity was assumed to be  $E_s = 200$  GPa (29 000 ksi), the strain at the onset of hardening was assumed to be  $\varepsilon_{sh} = 0.01$ , the uniform strain at the onset of necking was assumed to be  $\varepsilon_u = 0.1$ , and the elongation at fracture was assumed to be  $\varepsilon_f = 0.2$ . Reinforcing steel was modeled using an isotropic piecewise-linear plasticity model. Fracture of reinforcing bars was considered in both the interface beam elements and in the shell elements representing the floor slabs by defining a critical plastic strain at which the stress would drop to zero.

For concrete, the modulus of elasticity was calculated as  $E_c = 4700\sqrt{f'_c}$  MPa ( $E_c = 57000\sqrt{f'_c}$  psi). For unconfined concrete, the stress-strain relationship proposed by Popovics (1973) was adopted, as shown in Fig. 3(b), where the strain  $\varepsilon_{c1}$  was assumed to be 0.0022 and the cutoff strain  $n\varepsilon_{c1}$  is estimated according to the CEB-FIP model code (CEB 1991). To reduce spurious localization due to material softening, the appropriate value for the cutoff strain was calculated based on the element size to keep the compressive fracture energy  $G_{f,c}$  constant. As a result of the confinement provided by the transverse reinforcement, the core concrete has enhanced strength and ductility (see Fig. 3(b)). The modified Kent-Park model proposed by Scott et al. (1982) was used to represent the effects of confinement. For concrete in tension (Fig. 3(c)), a linear stress-strain relationship is used up to the tensile strength  $f_t$ , beyond which the stress is reduced linearly with increasing strain. The post-ultimate softening modulus accounts for the tension-stiffening effect, in which reinforcement holds the concrete together after initial cracking, allowing the concrete to continue to carry some tension as cracks open. The ultimate strain associated with crack opening,  $\varepsilon_u^{cr}$ , which controls the softening modulus, is calculated based on the tensile fracture energy  $G_{f,t}$  and the crack bandwidth  $h$ .

**Table 2. Expected-strength material properties used in analysis.**

Normal-weight concrete		ASTM A706 Grade 60 reinforcing bar	
Compressive strength, $f'_c$	Tensile strength, $f_t$	Yield strength, $f_y$	Tensile strength, $f_u$
41.4 MPa (6000 psi)	3.6 MPa (523 psi) *	517 MPa (75 ksi)	689 MPa (100 ksi)

\* Calculated based on compressive strength (CEB 1991).

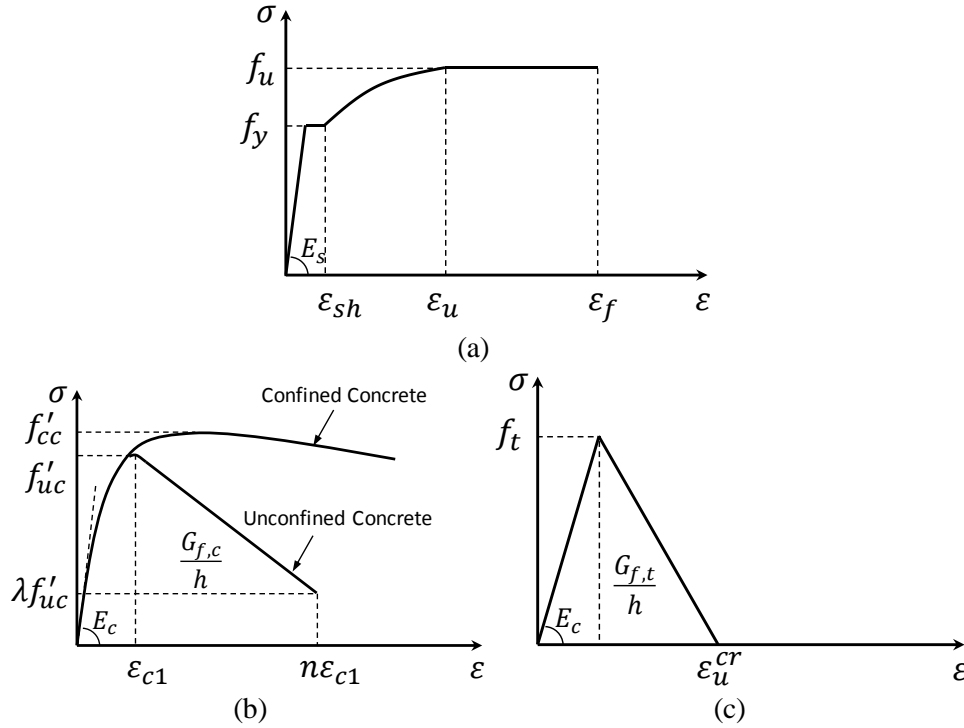


**Fig. 3. Typical material stress-strain relationships: (a) reinforcing bar; (b) concrete in compression; and (c) concrete in tension**

**Bond-slip effects.** Previous studies have indicated that the effects of bond-slip between concrete and reinforcing bars can be significant in computational simulations of reinforced concrete structures subject to column loss. If bond-slip is not considered, then bond-related failure modes cannot be captured, and the fully bonded assumption may result premature bar fracture due to strain localization at critical cross sections. In this study, bond-slip effects were considered in the interface elements at critical beam sections using the approach developed by Bao et al. (2014a), in which the stress-strain relationship of reinforcing bars is modified as follows:

$$\epsilon' = \frac{L-L_0}{L_0} = \frac{s(\sigma)+\epsilon L_0}{L_0} = s(\sigma) + f(\sigma) = f'(\sigma, L_0) \quad (1)$$

where  $s$  is the slip of the reinforcing bar at axial stress  $\sigma$ ,  $L_0$  is the original length of the reinforcing bar, and  $L$  is the deformed length of the reinforcing bar including slip. Further details on this approach for modeling bond slip were presented by Bao et al. (2014a).

The tension-stiffening effect is another important bond-related phenomenon in reinforced concrete members under tension. It is important to include the tension-stiffening effect for structural members subjected to tension throughout their cross-section, such as concrete slabs under membrane action. The tension-stiffening effect for concrete slabs is considered in this study through the post-ultimate softening modulus in the tensile response of concrete, as mentioned in the previous discussion of concrete material modeling.

## ALTERNATIVE LOAD PATH ANALYSIS OF PROTOTYPE BUILDING

Two types of ALPA examples are presented in this paper: nonlinear dynamic analysis and nonlinear static analysis. The former involves direct dynamic analysis of the structural response to sudden column loss. The latter involves a static pushdown analysis, using an energy-based procedure to account for dynamic effects associated with sudden column loss.

**Service-level gravity load.** The service-level gravity loading selected for the example analysis problems in the *ALPA Guidelines* is based on the following load combination, as specified in GSA (2003):

$$G = 1.0D + 0.25L \quad (2)$$

where  $D$  is the dead load and  $L$  is the live load. It is noted that ASCE 7-10 (ASCE 2010) specifies a load combination of  $1.2D + 0.5L$  for the residual capacity of structural systems following the notional removal of load-bearing elements. The load combination given by Eq. (2) is less conservative than that specified by ASCE 7-10, and it is noted the mean dead loads in modern construction typically correspond to a dead load factor of 1.05 or 1.10 (Ellingwood et al. 2007). Based on the gravity loads summarized in Table 1, Eq. (2) gives a combined gravity load of  $G = 9.82 \text{ kN/m}^2$  ( $205 \text{ lbf/ft}^2$ ) for typical floors and  $G = 7.96 \text{ kN/m}^2$  ( $166 \text{ lbf/ft}^2$ ) for the roof. These values of gravity loading were used in the analysis examples presented subsequently.

**Nonlinear dynamic analysis of sudden column loss.** Three individual column removal cases were considered in this study: the corner column A1, the edge column A3, and the interior column B3, all located at the first-story level. In the nonlinear dynamic analyses, the service-level gravity load  $G$  was first applied to the floor slabs, followed by sudden removal of the first-story column. In LS-DYNA, the sudden column removal was simulated by deleting the beam elements representing the corresponding column in a restart analysis of the building model loaded with the service-level gravity load  $G$ .

Fig. 4 shows contours of vertical displacement at the peak displacement after removal of the interior column B3 at the first-story level. Table 3 summarizes the structural responses of the prototype building under the three column loss scenarios. The prototype building remained stable for all column loss scenarios.

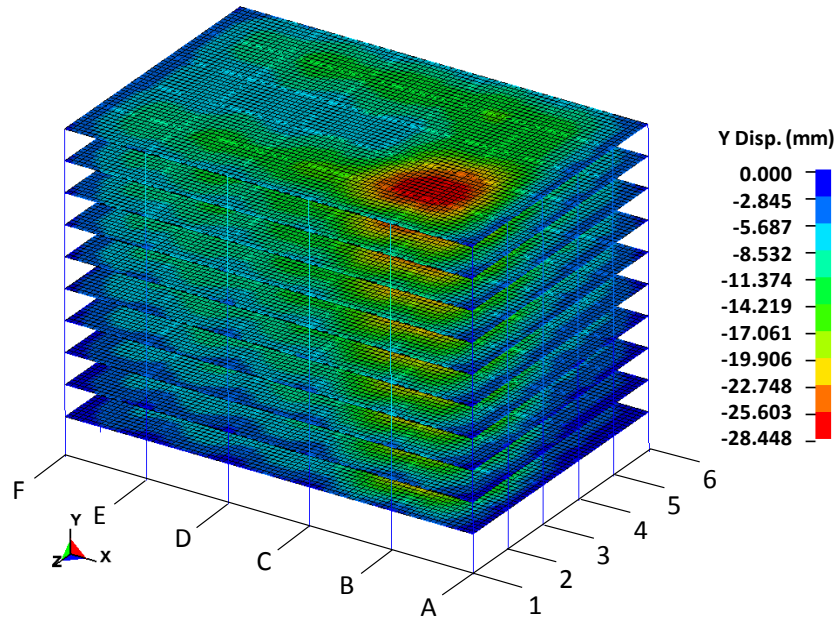


**Fig. 4. Vertical displacement contours at peak displacement after sudden loss of column B3**

**Table 3. Results from nonlinear dynamic analysis of sudden column loss.**

Column removal scenario	Final state of building	Peak displacement at removed column
Corner column A1	Stable	23 mm (0.90 in)
Edge column A3	Stable	19 mm (0.73 in)
Interior column B3	Stable	25 mm (0.96 in)

**Nonlinear static push-down analysis.** This section presents numerical procedures for structural robustness evaluation using nonlinear static push-down analysis. The loading scheme for a static push-down analysis is illustrated in Fig. 5, using the removal of column B3 as an example. The column is removed prior to application of gravity loading, and the service-level gravity loading  $G$  is first applied to the floor slab in bays unaffected by the column loss. Scaled gravity loading  $\lambda_s G$  is then applied to the bays adjoining the removed column, and the push-down analysis is performed by increasing the dimensionless factor  $\lambda_s$  from zero up to the ultimate load intensity that can be sustained by the structural system under the specified column loss scenario.

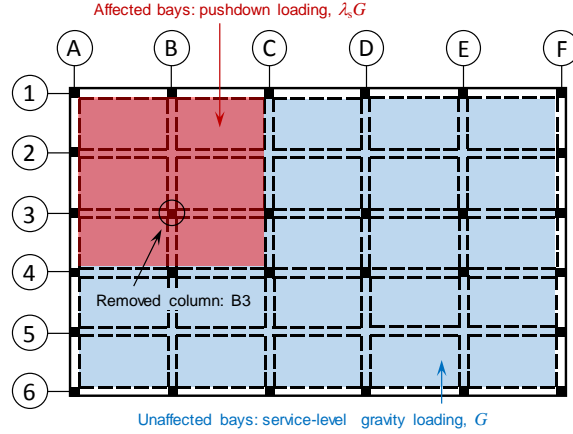


**Fig. 5. Loading scheme for push-down analysis: removal of column B3**

Fig. 6 shows the push-down curve obtained from nonlinear static analysis under removal of column B3, where the normalized load intensity  $\lambda_s$  is plotted against the vertical displacement at the removed column. As illustrated in Fig. 7, the collapse of the prototype building is initiated by failure of column B1 (circled in Fig. 7(a)), then progresses to the entire building (Fig. 7(b)). An approximate dynamic response curve, calculated from the static push-down curve based on the energy balance approach (Bao et al. 2014b, Main 2014, Izzuddin et al. 2008, Powell 2003), is also plotted along with the static response curve in Fig. 6. Each point on the approximate dynamic response curve relates the peak displacement at the removed column under sudden column loss with the corresponding load intensity applied to the affected bays. The normalized dynamic ultimate load intensity  $\lambda_{d,u}$  is defined as the dynamic load intensity at the displacement corresponding to the peak static load intensity  $\lambda_{s,u}$  (Main 2014; Bao et al. 2014b). A robustness index  $R$  is defined as the minimum value of the normalized ultimate capacity over all considered column removal scenarios:

$$R = \min_i (\lambda_{d,u}^i | i \in \text{considered column removal scenarios}) \quad (3)$$

Table 4 lists the normalized static and dynamic ultimate load intensities for the three column removal scenarios along with the corresponding dynamic increase factors (DIFs), which are obtained as the ratio,  $\lambda_{s,u}/\lambda_{d,u}$ . The robustness index  $R$  of the prototype building under the considered column removal scenarios is 1.54, which is greater than 1.0, indicating that no collapse would occur under the three column removal cases that were considered. Nonlinear dynamic analysis of the prototype building under the removal of column B3 was also performed under different levels of gravity loading, to verify the approximate dynamic responses calculated from the nonlinear static push-down analysis results. In the dynamic analyses, higher-intensity loads were applied to the affected bays and the service-level gravity load  $G$  is applied to the rest bays. The results from direct dynamic analysis are plotted along with the approximate dynamic response curve in Fig. 6, showing a reasonably consistent trend. Although the results from direct dynamic analysis indicate that the prototype building may avoid collapse under a load intensity beyond  $\lambda_{d,u}$ , the value of  $\lambda_{d,u}$  provides a conservative estimate for the largest normalized load intensity (1.80) that the prototype building can sustain without collapse under sudden column loss of column B3.

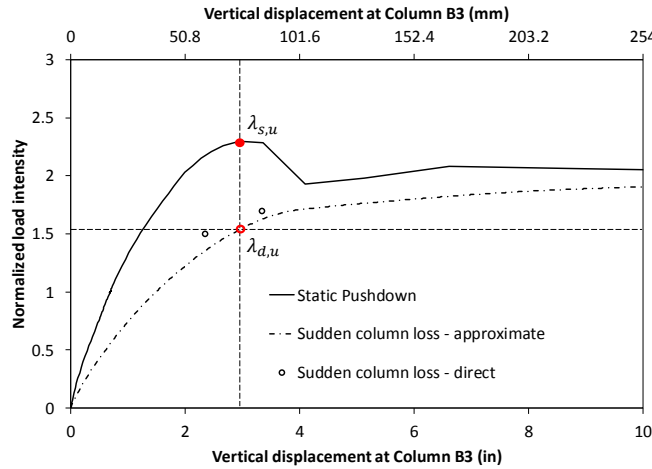


**Fig. 6. Analysis results for prototype building under loss of column B3**

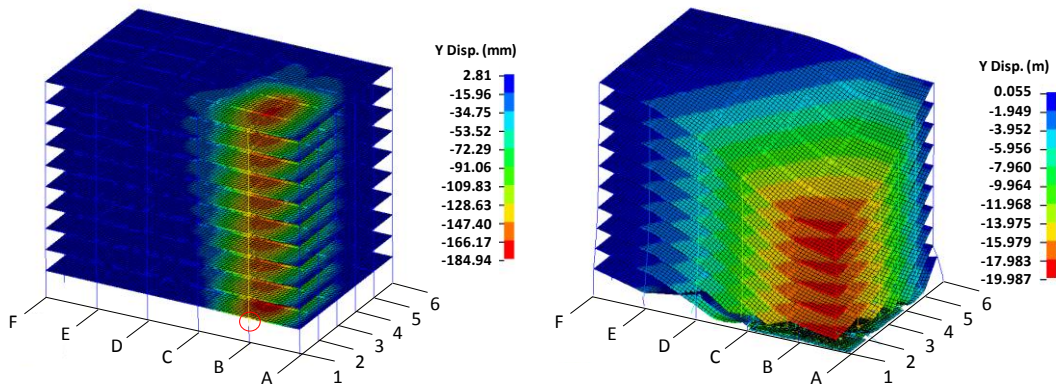


**Fig. 7. Contours of vertical displacement from nonlinear static push-down analysis under removal of column B3: (a) initial collapse due to failure of column B1; (a) progressive collapse under continued pushdown-loading.**

**Table 4. Results from nonlinear static push-down analysis.**

Column removal scenario	Static pushdown $\lambda_{s,u}$	Sudden column loss $\lambda_{d,u}$	Dynamic increase factor (DIF)
Corner column A1	5.06	4.24	1.19
Edge column A3	5.38	3.97	1.36
Interior column B3	2.30	1.54	1.49

## CONCLUDING REMARKS

Alternative load path analysis (ALPA) was performed for a 5-bay by 5-bay, 10-story prototype reinforced concrete moment frame building under three column loss scenarios: a corner column, an edge column and an interior column, all at the first-story level. The three column loss scenarios were analyzed using two types of ALPA analysis: nonlinear dynamic analysis and nonlinear static push-down analysis. No collapse was observed for the three column loss scenarios considered using either type of analysis. From the results of the nonlinear dynamic analysis, the largest vertical displacement at the removed column was 25 mm (0.96 in), which corresponded to the loss of interior column B3. From the results of the nonlinear static push-down analyses, loss of interior column B3 was also the most critical, with the lowest normalized capacity under static push-down loading of  $\lambda_{s,u} = 2.30$  and the lowest normalized capacity from approximate dynamic analysis of  $\lambda_{s,d} = 1.54$ . This latter value is the robustness index of the prototype building under the considered column removal scenarios. The approximate dynamic response calculated from push-down analysis using the energy-based approach was found to provide results that were reasonably consistent with nonlinear dynamic analysis. The predicted displacements from the approximate analysis tended to be larger than the displacements from nonlinear dynamic analysis under the same load intensity, and the approximate analysis gave conservative predictions of the ultimate capacity of the structural system under sudden column loss.

## REFERENCES

- American Society of Civil Engineers (ASCE). (2002). "Minimum design loads for buildings and other structures." *SEI/ASCE 7-02*, Reston, VA.
- American Society of Civil Engineers (ASCE). (2010). "Minimum design loads for buildings and other structures." *SEI/ASCE 7-10*, Reston, VA.
- American Society of Civil Engineers (ASCE). (2013). "Seismic evaluation and retrofit of existing buildings." *ASCE/SEI 41-13*, Reston, VA.
- American Concrete Institute (ACI). (2002). "Building code requirements for structural concrete and commentary." *ACI 318-02 and ACI 318R-02*, Farmington Hills, MI.
- Bao, Y., Lew, H.S., and Kunnath, S. (2014a). "Modeling of reinforced concrete assemblies under a column removal scenario," *J. Struct. Eng.*, 140(1), 04013026.
- Bao, Y., Main, J.A., Lew, H.S., and Sadek, F. (2014b). "Robustness assessment of RC frame buildings under column loss scenarios." *Proc., ASCE/SEI Structures Congress 2014*, Boston, MA.
- Comite Euro-International du Beton (CEB). (1991). *CEB-FIP Model Code 1990 Design Code*, Published by Thomas Telford, London, UK.
- Ellingwood, B.R., Smilowitz, R., Dusenberry, D.O., Duthinh, D., Lew, H.S., and Carino, N.J. (2007). "Best practices for reducing the potential for progressive collapse in buildings." *NISTIR 7396*, National Institute of Standards and Technology, Gaithersburg, MD.

- General Services Administration (GSA). (2003). "Progressive collapse analysis design guidelines for new federal office buildings and major modernization projects." Washington, DC.
- Hallquist, J. (2007). "LS-DYNA keyword user's manual." Livermore Software Technology Corporation, Livermore, CA.
- International Code Council (ICC). (2003). *International Building Code*, Falls Church, VA.
- Izzuddin, B.A., Vlassis, A.G., Elghazouli, A.Y., and Nethercot. D.A. (2008). "Progressive collapse of multi-storey buildings due to sudden column loss – Part I: Simplified assessment framework." *Eng. Struct.*, 30, 1308-1318.
- Livermore Software Technology Corporation (LSTC). (2014). *LS-DYNA, a program for nonlinear dynamic analysis of structures in three dimensions, Version R7.1.1*, Livermore, CA.
- Main, J.A. (2014). "Composite floor systems under column loss: collapse resistance and tie force requirements." *J. Struct. Eng.*, 140, Special Issue: Computational Simulation in Structural Engineering, A4014003.
- Popovics, S. (1973). "A numerical approach to the complete stress strain curve for concrete." *Cement and Concrete Research*, 3(5), 583-599.
- Powell, G. (2003). "Collapse analysis made easy (more or less)." *Proc., Annual Meeting of the Los Angeles Tall Buildings Structural Design Council: Progressive collapse and blast resistant design of buildings*, Los Angeles, CA.
- Scott, B.D., Park, R., and Priestley, M.J.N. (1982). "Stress-strain behavior of concrete confined by overlapping hoops at low and high strain rates." *ACI J.*, 79(1), 13-27.
- Shen, Q. and Ghosh, S.K. (2006). "Assessing ability of seismic structural systems to withstand progressive collapse: Progressive collapse analysis of cast-in-place concrete frame buildings." *Report submitted to the Building and Fire Research Laboratory*, NIST, Gaithersburg, MD.